BIOCHEMISTRY
including biophysical chemistry & molecular biology

Article

pubs.acs.org/biochemistry

Isotope Effects for Deuterium Transfer and Mutagenesis of Tyr187 Provide Insight into Controlled Radical Chemistry in Adenosylcobalamin-Dependent Ornithine 4,5-Aminomutase

Caitlyn Makins,[†] Doug A. Whitelaw,[†] Changhua Mu,[‡] Charles J. Walsby,[‡] and Kirsten R. Wolthers*[,†]

[†]Department of Chemistry, University of British Columbia, 3333 University Way, Kelowna, BC V1V 1V7, Canada

[‡]Department of Chemistry, Simon Fraser University, 8888 University Drive, Burnaby, BC V5A 1S6, Canada

Supporting Information

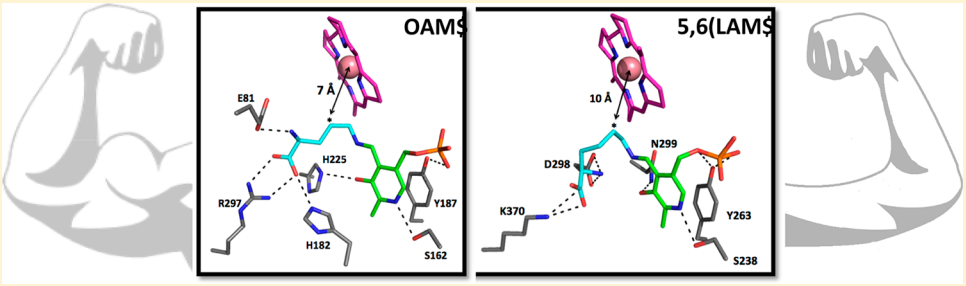

ABSTRACT: Adenosylcobalamin-dependent ornithine 4,5-aminomutase (OAM) from *Clostridium sticklandii* utilizes pyridoxal 5′-phosphate (PLP) to interconvert D-ornithine to 2,4-diaminopentanoate via a multistep mechanism that involves two hydrogen transfer steps. Herein, we uncover features of the OAM catalytic mechanism that differentiate it from its homologue, the more catalytically promiscuous lysine 5,6-aminomutase. Kinetic isotope effects (KIEs) with DL-ornithine-3,3,4,4,5,5-d_6 revealed a diminished $^{D}k_{cat}/K_m$ of 2.5 ± 0.4 relative to a $^{D}k_{cat}$ of 7.6 ± 0.5, suggesting slow release of the substrate from the active site. In contrast, a KIE was not observed on the rate constant associated with Co−C bond homolysis as this step is likely "gated" by the formation of the external aldimine. The role of tyrosine 187, which lies planar to the PLP pyridine ring, was also investigated via site-directed mutagenesis. The 25- and 1260-fold reduced k_{cat} values for Y187F and Y187A, respectively, are attributed to a slower rate of external aldimine formation and a diminution of adenosylcobalamin Co−C bond homolysis. Notably, electron paramagnetic resonance studies of Y187F suggest that the integrity of the active site is maintained as cob(II)alamin and the PLP organic radical (even at lower concentrations) remain tightly exchange-coupled. Modeling of D-lysine and L-β-lysine into the 5,6-LAM active site reveals interactions between the substrate and protein are weaker than those in OAM and fewer in number. The combined data suggest that the level of protein−substrate interactions in aminomutases not only influences substrate specificity, but also controls radical chemistry.

Adenosylcobalamin (AdoCbl, coenzyme B_{12})-dependent isomerases catalyze chemically and energetically difficult rearrangements through the use of radicals. The isomerization reaction is a 1,2-rearrangement whereby a hydrogen atom and a variable substituent on an adjacent carbon atom are interchanged.[1,2] Ornithine 4,5-aminomutase (OAM) and lysine 5,6-aminomutase (5,6-LAM) are currently the only known AdoCbl-dependent isomerases that utilize an additional cofactor, pyridoxal 5′-phosphate (PLP), for catalysis. Both enzymes function in the catabolism of amino acids in several species of anaerobic bacteria, most notably *Clostridia*.[3] OAM is highly substrate specific for D-ornithine, which it interconverts to 2,4-diaminopentanoate (DAP).[4] In contrast, 5,6-LAM shows more substrate promiscuity as it is able to transform D- or L-lysine into D- or L-2,5-diaminohexanoate, respectively, as well as L-β-lysine into 3,5-diaminohexanoate.[5,6]

Ornithine 4,5-aminomutase and lysine 5,6-aminomutase display several structural similarities. OAM is an $\alpha_2\beta_2$ heterodimer comprised of two strongly associating subunits, OraE (82.9 kDa) and OraS (12.8 kDa).[7] Each OraE subunit comprises a triosephosphate isomerase (TIM) barrel domain and a Rossmann-like domain. A domain swap occurs in the heterodimer, whereby the Rossmann-like domain of one OraE subunit associates with the TIM barrel domain of a second OraE subunit and vice versa, such that two identical active sites are formed.[8] 5,6-LAM is also an $\alpha_2\beta_2$ heterodimer; however, unlike OAM, the TIM barrel and Rossmann-like domains are found on separate α (55 kDa) and β (30 kDa) subunits. The α and β subunits have sequences 28 and 35% identical and 39 and 47% similar, respectively, to that of the OraE subunit of OAM.[9] In both enzymes, the Rossmann-like domain, which houses the AdoCbl cofactor, and the TIM barrel domain, which houses the

Received: May 30, 2014
Revised: July 23, 2014
Published: August 6, 2014

   dx.doi.org/10.1021/bi5006706 | *Biochemistry* 2014, 53, 5432−5443

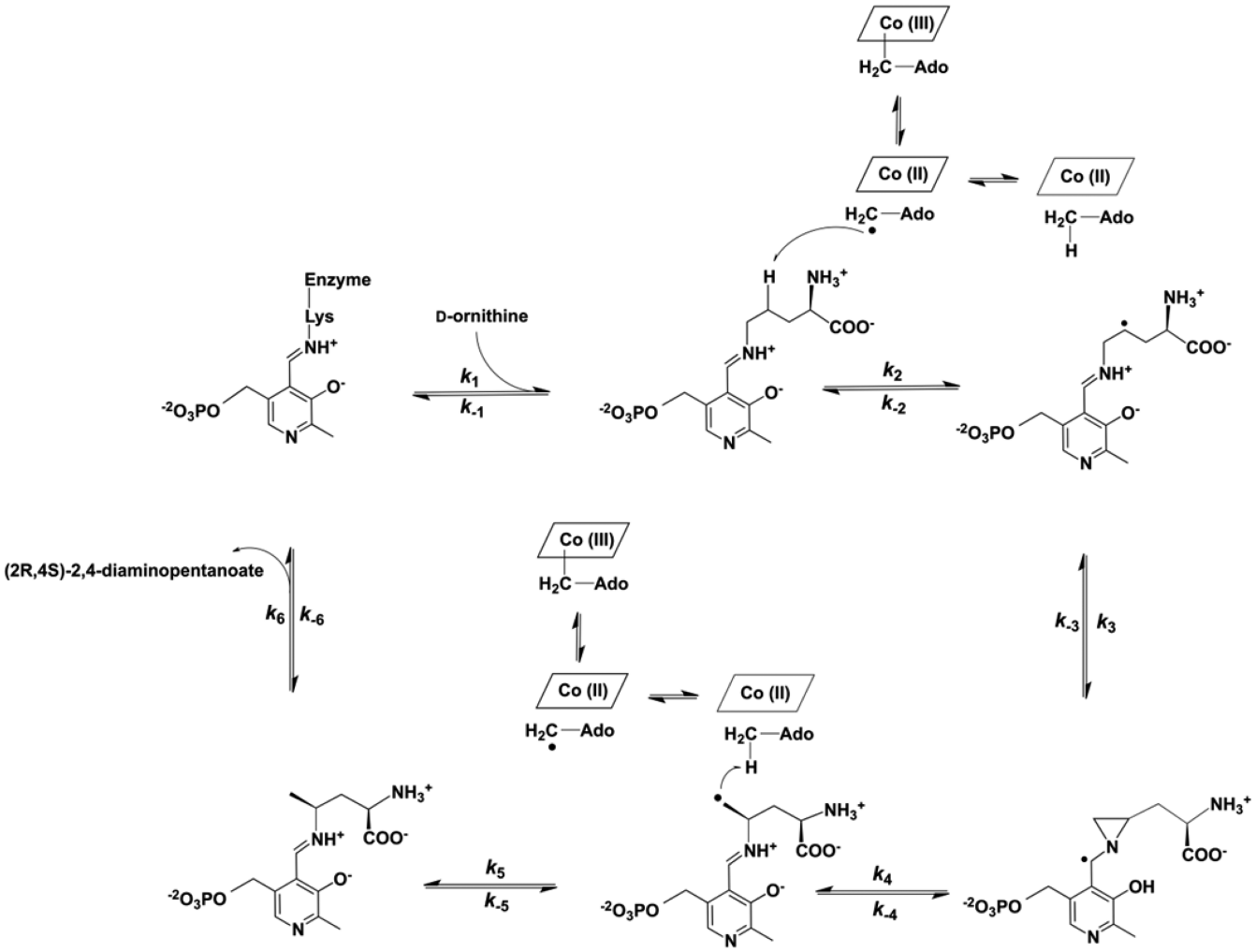

Figure 1. Proposed catalytic mechanism for ornithine 4,5-aminomutase. Binding of the substrate results in transimination, whereby the internal aldimine linkage between PLP and Lys629 is replaced by an external aldimine linkage between PLP and the terminal amino group of D-ornithine. Conformational changes upon substrate binding induce homolysis of the AdoCbl Co−C bond, resulting in the formation of cob(II)alamin and a 5′-deoxyadenosyl radical (Ado$^{\bullet}$). Ado$^{\bullet}$ abstracts the C4 hydrogen from D-ornithine to form a substrate radical intermediate and 5′-deoxyadenosine. The substrate radical then isomerizes into a productlike radical via an azacyclopropylcarbinyl radical intermediate. Re-abstraction of a hydrogen atom from 5′-deoxyadenosine by the productlike radical regenerates the adenosyl radical. Product release and recombination of Ado$^{\bullet}$ with cob(II)alamin to re-form the Co−C bond complete the catalytic cycle.

PLP cofactor, are held together in an "edge-on" conformation secured by an imine (Schiff base) linkage between PLP and a lysine residue (Lys144β in 5,6-LAM and Lys629 in OAM) within the Rossmann-like domain.[8,10] The "edge-on" conformation enforces a distance of 23 Å, which ostensibly protects the enzyme from spurious radical generation in the absence of substrate.

The proposed catalytic mechanism for AdoCbl-dependent aminomutases (Figure 1) is based on *S*-adenosyl-L-methionine- and PLP-dependent lysine 2,3-aminomutase, which catalyzes a similar 1,2-amino group migration.[11−14] Substrate binding results in the formation of an external aldimine between PLP and the terminal amino group of the substrate. This initial catalytic step frees the Rossmann-like domain to rotate and position itself directly over the TIM barrel domain in a conformation similar to that captured in the crystal structures of glutamate mutase and methylmalonyl-CoA mutase.[15,16] This "top-on" conformation establishes new noncovalent interactions between the adenosyl moiety and active site residues, which contribute to homolysis of the AdoCbl Co−C bond resulting in the formation of cob(II)alamin and a 5′-deoxyadenosyl radical (Ado$^{\bullet}$).[17] Ado$^{\bullet}$ abstracts a hydrogen atom from the substrate to form a substrate radical intermediate and 5′-deoxyadenosine (AdoH). The substrate radical then isomerizes into a productlike radical via an azacyclopropylcarbinyl radical intermediate. Re-abstraction of a hydrogen atom from AdoH by the productlike radical regenerates the adenosyl radical. The catalytic cycle is complete with product release and recombination of Ado$^{\bullet}$ with cob(II)alamin to re-form the Co−C bond.

Apart from its role in anchoring the substrate within the active site, computational studies indicate that the PLP lowers the barrier to intramolecular isomerization by introducing unsaturation into the migrating amino group. This allows isomerization of the substrate radical to proceed via a cyclic intermediate, which is stabilized through captodative effects.[18] Residues proximal to the PLP cofactor are likely to further modulate radical stability and catalysis (Figure 2). For example, a tyrosine residue (Y263α) in 5,6-LAM, which forms a π-stacking interaction with the pyridine ring of PLP, was recently

dx.doi.org/10.1021/bi5006706 | *Biochemistry* 2014, 53, 5432−5443

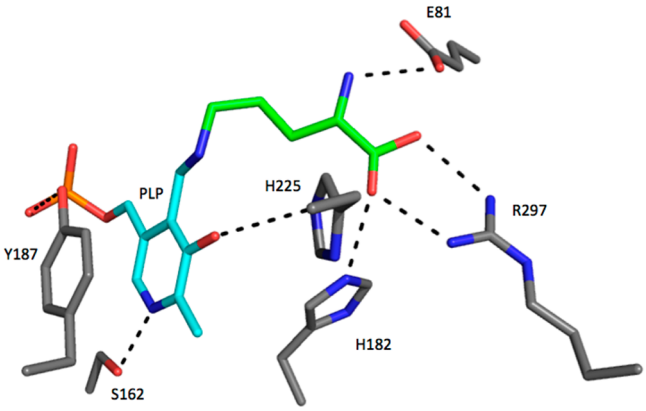

Figure 2. Active site of ornithine 4,5-aminomutase complexed with the natural substrate D-ornithine (Protein Data Bank entry 3KOZ). The substrate (green) forms a covalent Schiff base linkage with the imine nitrogen of the PLP cofactor (cyan). Selected active site residues interacting with the substrate and PLP cofactor are colored gray. In particular, Tyr187 forms a π-stacking interaction with the pyridine ring of PLP, the guanidinium side chain of Arg297 forms a salt bridge with the α-carboxylate group of the substrate, and residues His225, His182, Asn226, Glu81, and Ser162 provide additional hydrogen bonding interactions with the substrate and cofactor.

implicated in stabilizing the azacyclopropylcarbinyl radical intermediate, as well as protecting the enzyme from inactivation by molecular oxygen.[19]

The goal of this work is to provide a more thorough kinetic analysis of the catalytic mechanism of OAM, allowing us to draw comparisons with 5,6-LAM. To do so, we have mutated OAM Y187, the residue analogous to Y263α of 5,6-LAM, to a Phe and an Ala to assess its role in OAM catalysis using UV–visible and electron paramagnetic resonance (EPR) spectroscopies. In addition, we have performed steady-state and pre-steady-state kinetic isotope effect experiments with native OAM and the Y187 variants. The only crystal structure available for 5,6-LAM is a substrate-free form; therefore, docking experiments were performed to generate models of the 5,6-LAM active site with bound D-lysine and L-β-lysine. Our results show that mutation of Y187 is less deleterious in OAM than in 5,6-LAM, which may be linked to differences in the active site architecture and catalytic behaviors of the two enzymes.

EXPERIMENTAL PROCEDURES

Materials. AdoCbl, PLP, D-ornithine, L-ornithine, and DL-2,4-diaminobutyric acid were obtained from Sigma. L-Ornithine-3,3,4,4,5,5-d_6 hydrochloride and D-2,4-diaminobutyric-2,3,3,4,4-d_5 acid dihydrochloride were obtained from C/D/N Isotopes Inc. The Ni^{2+}-nitrilotriacetic acid (Ni-NTA) column and Q-Sepharose High Performance resins were from GE Biosciences. Restriction endonucleases were from New England Biolabs; *Pfu* Turbo DNA polymerase was from Agilent Technologies, and Rosetta(DE3)pLysS competent cells were purchased from EMD Biosciences. All other chemicals were purchased from Fisher Scientific and were of the highest grade available.

Cloning and Expression of Ornithine Racemase. The gene sequence encoding ornithine racemase (OR) was amplified via polymerase chain reaction (PCR) from *Clostridium difficile* (Hall and O'Toole) Prevot (ATCC BAA-1382D-5) genomic DNA with *Pfu* DNA polymerase. The forward and reverse primers were 5′-CAT AAG TAG **CAT ATG** TAT CCT AGG TTA GAA ATA G-3′ (NdeI restriction site in bold) and 5′-TGA TAC CAT **AAG CTT** CAC TAT AAT TTT TTT TGC AAC ATA TTT GC-3′ (HindIII restriction site in bold), respectively. The PCR product was digested with NdeI and HindIII and then ligated into the pET-41a vector (EMD Biosciences) also cut with the same restriction enzymes. The resulting plasmid, designated pET-OR, was transformed into *Escherichia coli* XL1-blue cells (Agilent Technologies). Sequencing by the NAPS DNA Sequencing Laboratory at the University of British Columbia (Vancouver, BC) confirmed the absence of any PCR-induced errors. The pET-OR plasmid was then transformed into *E. coli* Rosetta(DE3)pLysS cells for overexpression of the protein. A single colony was used to inoculate 5 mL of Luria-Bertani (LB) broth containing 100 μg/mL ampicillin and 34 μg/mL chloramphenicol. The culture was grown for 8 h at 37 °C, transferred to 200 mL of LB broth containing the same antibiotics, and then grown at 37 °C for 16 h. Ten milliliters of the 200 mL starter culture was used to inoculate 0.5 L of TB containing ampicillin (100 μg/mL) and chloramphenicol (34 μg/mL), which was then grown at 30 °C until an OD_{600} of 1.0 was reached, at which point the cells were induced with 0.1 mM isopropyl β-D-1-thiogalactopyranoside and then grown for an additional 16 h at 20 °C. The cells were pelleted and stored at −80 °C.

Construction of OAM Variants. The Y187F and Y187A single-point mutations were introduced into the pOAMH2 vector[20] using the QuikChange site-directed mutagenesis kit (Agilent Technologies, Mississauga, ON). The NAPS DNA Sequencing Laboratory at the University of British Columbia confirmed the presence of the mutations and the absence of any other PCR-induced errors.

Enzyme Purification. Wild-type OAM and 2,4-diaminopentanoate dehydrogenase (DAPDH) were purified as previously described.[20,21] The following protocol was used for the preparation of ornithine racemase. All purification steps were conducted at 4 °C. Cells overexpressing ornithine racemase (50 g, wet weight) were resuspended in 250 mL of 50 mM Tris (pH 7.5) containing the protease inhibitors benzamidine (2 mM) and phenylmethanesulfonyl fluoride (1 mM). The mixture was then sonicated (8 s pulses every minute for 45 min, power setting of 21%) using a Misonix sonicator, followed by centrifugation at 25000*g* for 45 min to remove cellular debris. Upon addition of NaCl and imidazole to final concentrations of 0.5 M and 20 mM, respectively, the crude extract was run over a 5 mL HisTrap-FF column (GE Biosciences) equilibrated with 50 mM Tris (pH 7.5), 0.5 M NaCl, and 20 mM imidazole. The protein was eluted with 300 mM imidazole. Fractions containing the enzyme (yellow in color) were pooled and dialyzed against 50 mM Tris (pH 7.5), 1 mM EDTA, and 2 mM β-mercaptoethanol for 2 h at 4 °C. The dialysate was concentrated [Vivaspin 20, 30 kDa molecular weight cutoff (MWCO)] and then further diluted with 50 mM Tris (pH 7.5) to decrease the concentration of NaCl. The protein was then loaded onto a 58 mL Q-Sepharose HP column (2.6 cm × 11 cm) equilibrated with 50 mM Tris (pH 7.5). After the application of the protein, the column was washed with 120 mL of 50 mM Tris (pH 7.5) and eluted with a linear gradient from 0 to 500 mM NaCl. Fractions containing the enzyme were pooled and concentrated. A Lowry assay, using bovine serum albumin as a standard, was performed to determine the concentration of ornithine racemase. After 20%

dx.doi.org/10.1021/bi5006706 | *Biochemistry* 2014, 53, 5432−5443

glycerol stocks had been made, the enzyme was flash-frozen in liquid nitrogen and stored at −80 °C.

Preparation of DL-Ornithine and DL-Ornithine-3,3,4,4,5,5-d_6. Ornithine racemase was used to synthesize a racemic mixture of DL-ornithine from L-ornithine using the following procedure. A 10 mL solution containing 100 mM L-ornithine and 10 μM ornithine racemase (pH 8.0) was stirred gently for 18 h at 20 °C (pH monitored periodically). Aluminum foil was wrapped around the reaction flask to minimize exposure of the pyridoxal 5′-phosphate cofactor to ambient light. The reaction mixture was passed through a 30 kDa MWCO filter, to remove the enzyme, and then dried under reduced pressure. The resulting solid was washed with ethanol and then dried under reduced pressure, leaving behind a fine white powder. ^{1}H nuclear magnetic resonance (NMR) was used to confirm the purity of the ornithine product. The same procedure was used to synthesize DL-ornithine-3,3,4,4,5,5-d_6 from L-ornithine-3,3,4,4,5,5-d_6.

Coupled Enzyme Assays. The activity of wild-type OAM and the OAM variants toward DL-ornithine and DL-ornithine-3,3,4,4,5,5-d_6 was measured using a coupled spectrophotometric assay with DAPDH, as previously described.[21] Initial rates were plotted as a function of substrate concentration and fit to the Michaelis−Menten equation using Origin, version 8.5 (MicroCal Software Inc.). The coupled enzyme assay was also used to verify that purified ornithine racemase was active. For this assay, ornithine racemase (1 nM) was combined with excess OAM (2 μM), DAPDH (1 μM), and NAD^+ (2 mM) in 100 mM NH_4^+EPPS buffer (pH 8.5) in a 1 mL reaction volume. The reaction was initiated with 20 mM L-ornithine. The conversion of L-ornithine to D-ornithine by ornithine racemace was monitored by following the absorbance increase at 340 nm, signifying the reduction of NAD^+ to NADH by DAPDH.

Determination of the Equilibrium Constant. The equilibrium constant for the reaction of wild-type OAM with D-ornithine was determined using ^{1}H NMR spectroscopy. An equimolar mixture (2 μM) of apo-OAM, AdoCbl, and PLP in 20 mM Tris (pH 8.5) was reacted with 5 mM D-ornithine in the dark under anaerobic conditions for 18 h at 25 °C. The sample was then lyophilized, reconstituted in D_2O, and then analyzed on a 400 MHz Varian Mercury VX spectrometer at 298 K. The relative integrals were compared for the protons on C5 of D-ornithine and the product DAP, corrected to their relative number of protons.

Aerobic UV−Visible Spectroscopy. Aerobic spectral assays were conducted on a PerkinElmer Lambda 25 spectrophotometer at 25 °C. Each 1 mL reaction mixture contained 15 μM apo-OAM, 15 μM PLP, and 15 μM AdoCbl in 100 mM NH_4^+EPPS buffer (pH 8.5). Each reaction was initiated via the addition of 2.5 mM DL-2,4-diaminobutyrate or D-ornithine, and scans were collected from 700 to 300 nm every minute for 30 min.

Anaerobic UV−Visible Spectroscopy. Anaerobic spectral binding studies were conducted in a Belle Technology glovebox under low-ambient light conditions. The concentrated enzyme was gel-filtered over a 10 mL PD10 column equilibrated with 100 mM NH_4^+EPPS (pH 8.5), free of O_2. Powdered forms of the cofactors, substrate, and inhibitor were introduced into the glovebox and dissolved in anaerobic buffer prior to use. Each 1 mL mixture contained 40 μM apo-OAM, 40 μM PLP, and 40 μM AdoCbl in 100 mM NH_4^+EPPS (pH 8.5). A scan from 700 to 300 nm was taken prior to and 10 min after the addition of 2.5 mM DL-2,4-diaminobutyrate acid or D-ornithine.

Stopped-Flow Spectroscopy. Stopped-flow studies were performed using an SF-61DX2 stopped-flow instrument (TgK Scientific), under anaerobic conditions where the O_2 concentration was maintained at <5 ppm. Anaerobic solutions of buffer, enzyme, cofactors, substrate, and substrate analogues were prepared as previously described.[20] An equimolar mixture (50 μM) of apoOAM, PLP, and AdoCbl was rapidly mixed with 5 mM D-ornithine or DL-2,4-diaminobutyrate. The transimination and Co−C bond homolysis events were followed at 416 and 528 nm, respectively. All experiments were conducted at 25 °C except those with the wild-type enzyme, which were performed at 6.7 °C to catch more of the homolysis absorbance trace. An average of 8−10 traces were fit to a monoexponential equation to determine the observed rate constants.

EPR Spectroscopy. Approximately 2 mL of a protein sample (20 mg/mL) was introduced into the anaerobic glovebox and gel-filtered over a PD10 column equilibrated with 100 mM NH_4^+EPPS (pH 8.5). The filtered sample was then concentrated under anaerobic conditions to >0.6 mM using a Vivaspin 500 centrifugal concentrator with a 30 kDa MWCO (GE Biosciences). Powdered forms of the cofactors, substrate, and inhibitor were introduced into the glovebox and dissolved in anaerobic buffer prior to use. An equimolar mixture (600 μM) of enzyme, PLP, and AdoCbl was prepared and allowed to incubate for 5 min. After the addition of either 5 mM D-ornithine or DL-2,4-diaminobutyrate, the samples were mixed thoroughly, loaded into EPR tubes, and frozen in liquid nitrogen. All sample preparation steps were conducted anaerobically at 25 °C under low-light conditions to minimize photolysis of the AdoCbl Co−C bond. EPR spectra were measured on a Bruker EMXplus spectrometer with a PremiumX microwave bridge and HS resonator at X-band (9.38 GHz) at 77 K. The experimental EPR spectrum was simulated using EasySpin[22] following a strategy similar to that outlined by Bothe et al.[23]

Substrate Docking Simulations. Molecular docking simulations were conducted using AutoDock version 4.2.5.1 obtained from the Scripps Research Institute (La Jolla, CA). The starting coordinates for lysine 5,6-aminomutase [Protein Data Bank (PDB) entry 1XRS][10] were obtained from the PDB. Because substrate binding results in the breakage of a covalent bond between the enzyme and the PLP cofactor, followed by formation of a new covalent bond between PLP and the substrate, the PLP cofactor coordinates were removed from the original PDB file. The PLP−substrate adduct was then modeled into the active site of the enzyme. Given that 5,6-LAM accepts both D-lysine and L-β-lysine, input files for PLP- D-lysine and PLP- L-β-lysine were generated with hydrogen atoms using ChemBio3D Ultra version 12.0 (CambridgeSoft Corp., Cambridge, MA). Both input files were energy minimized using MM2 prior to running AutoDock.

AutoDock Tools was used to prepare the ligand and rigid receptor coordinate files for the two docking simulations. Hydrogen atoms were added to the receptor, and Gasteiger partial atomic charges were assigned to the ligand and the receptor. In both simulations, 10 of the possible 12 torsions in the respective ligand were active to preserve the intramolecular hydrogen bond, which exists between the imine nitrogen and the hydroxyl group of the pyridine ring. The search space was confined to a 22.5 Å × 22.5 Å × 22.5 Å box centered at 57.000, 42.000, and 80.101 to include the site of the original PLP

dx.doi.org/10.1021/bi5006706 | Biochemistry 2014, 53, 5432−5443

Table 1. Summary of Steady-State Kinetic Parameters for k_{cat} and k_{cat}/K_m for Wild-Type OAM and the Y187 Variants with Substrate DL-Ornithine and Observed Kinetic Isotope Effects upon Reaction with Deuterium-Labeled Substrate DL-Ornithine-3,3,4,4,5,5-d_6

enzyme	k_{cat} (s^{-1})	K_m (μM)	k_{cat}/K_m (M^{-1} s^{-1})	$^{D}k_{cat}$	$^{D}k_{cat}/K_m$
wild type	2.9 ± 0.1	567 ± 45	5120 ± 410	7.6 ± 0.5	2.5 ± 0.4
Y187F	(1.15 ± 0.01) × 10^{-1}	162 ± 5	710 ± 28	16.7 ± 0.4	5.3 ± 0.6
Y187A	(2.3 ± 0.1) × 10^{-3}	68 ± 6	34 ± 5	2.7 ± 0.2	ND[a]

[a]Because of the slow rate of turnover, we were unable to determine a value of $^{D}k_{cat}/K_m$ for the Y187A mutant.

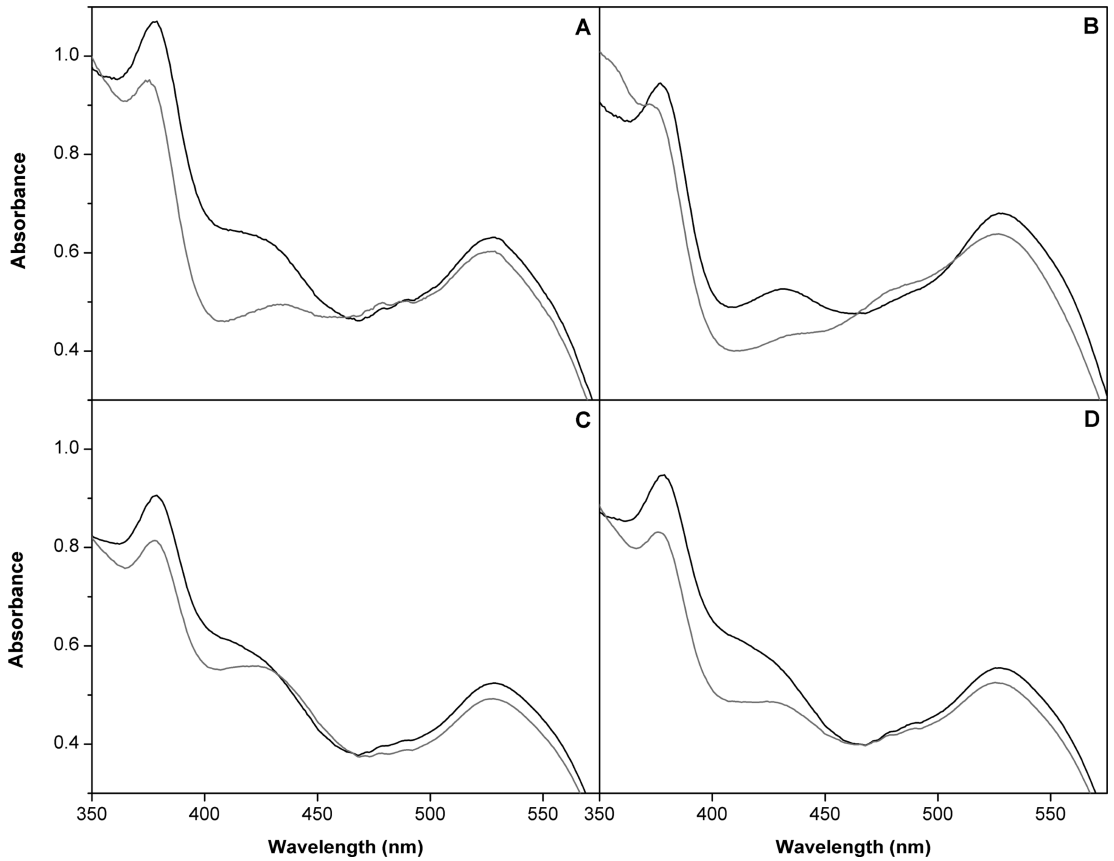

Figure 3. Anaerobic binding spectra of the Y187 variants. The holoenzyme solution contained 40 μM OAM, 40 μM PLP, and 40 μM AdoCbl in 100 mM NH_4^+EPPS (pH 8.5). Spectral changes for Y187F (A and B) and Y187A (C and D) were recorded before (black line) and 10 min after (gray line) the addition of 2.5 mM D-ornithine (A and C) and the inhibitor DL-2,4-diaminobutyric acid (B and D).

cofactor. One hundred structures were generated using the Lamarkian genetic algorithm. Default parameters were used and the number of energy evaluations was set to 250000. Solution structures were clustered according to their conformational similarities and then ranked from lowest to highest energy within each cluster.

RESULTS

Purification of Ornithine Racemase. PLP-dependent ornithine racemase, the first enzyme in the anaerobic oxidative degradation pathway of L-ornithine, converts L-ornithine to D-ornithine.[24] DL-Ornithine-3,3,4,4,5,5-d_6 was enzymatically produced from L-ornithine-3,3,4,4,5,5-d_6 using ornithine racemase cloned from *C. difficile* genomic DNA. Ornithine racemase, bearing a C-terminal hexahistidine tag, was heterologously expressed in *E. coli* and purified to homogeneity via Ni-NTA affinity chromatography followed by anion exchange chromatography. The apparent molecular mass (42 kDa), as determined by sodium dodecyl sulfate−polyacrylamide gel electrophoresis, closely matches the predicted molecular mass of 41772 kDa for a hexahistidine-tagged OR (Figure S1).

Determination of the Equilibrium Constant for OAM. Reaction of D-ornithine with OAM results in a shift of the terminal amino group from C5 to C4 to produce 2,4-diaminopentanoate. The two hydrogen atoms on C5 of D-ornithine appear as a triplet at 3.02 ppm (J = 7.4 Hz) in a ^{1}H NMR spectrum, while the three hydrogen atoms on C5 of the product 2,4-diaminopentanoate appear as a doublet at 1.33 ppm (J = 6.6 Hz). Using the relative integrals of these peaks, the equilibrium constant for OAM was determined to be 1.71, indicating that the reaction is reversible, with a slight preference for product formation.

Deuterium Kinetic Isotope Effects for OAM and the OAM Variants. The kinetic parameters for wild-type OAM and the Tyr187 variants with DL-ornithine along with the observed isotope effects with DL-ornithine-3,3,4,4,5,5-d_6 are summarized in Table 1 and Table S1 of the Supporting Information. Wild-type OAM displayed a catalytic turnover rate

dx.doi.org/10.1021/bi5006706 | Biochemistry 2014, 53, 5432−5443

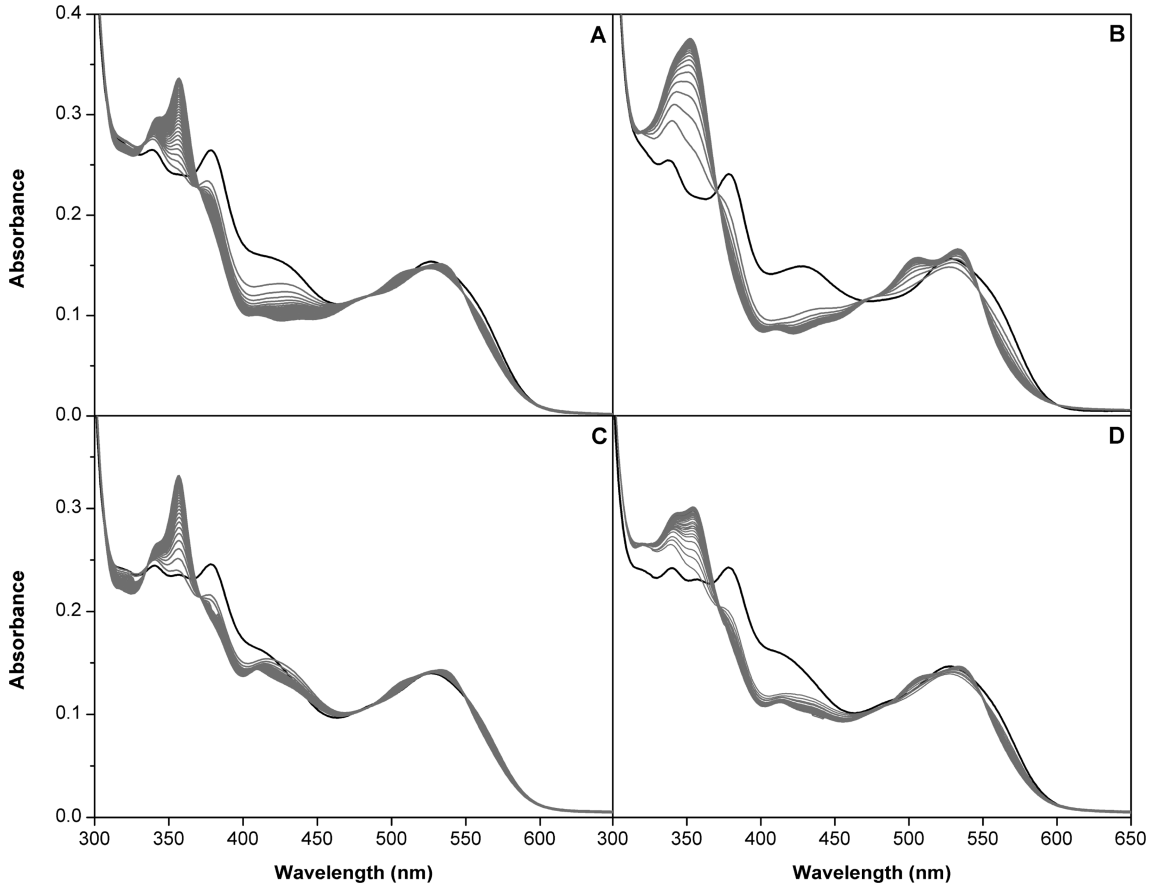

Figure 4. Aerobic binding spectra of the Y187 variants. The holoenzyme solution contained 15 μM OAM, 15 μM PLP, and 15 μM AdoCbl in 100 mM NH_4^+EPPS (pH 8.5). Spectral changes for Y187F (A and B) and Y187A (C and D) were recorded prior to the addition of the substrate (black lines) and then every minute for 30 min (gray lines) following the addition of 2.5 mM D-ornithine (A and C) and 2.5 mM DL-2,4-diaminobutyric acid (B and D).

of 2.9 ± 0.1 s^{-1} and a K_m value of 567 ± 45 μM for DL-ornithine; similar values were previously obtained with enantiopure D-ornithine.[21] Both k_{cat} and K_m for wild-type OAM were reduced with DL-ornithine-3,3,4,4,5,5-d_6, resulting in a $^{D}k_{cat}$ value of 7.6 ± 0.5 and a $^{D}k_{cat}/K_m$ value of 2.5 ± 0.4. The suppression of the KIE in $^{D}k_{cat}/K_m$ relative to the value of $^{D}k_{cat}$ suggests that OAM has a large forward commitment to catalysis, likely because of slow release of the substrate from the active site.

Mutation of Tyr187 to a Phe resulted in a 25-fold decrease in the rate of catalytic turnover and a 7-fold decrease in the overall catalytic efficiency. Complete removal of the phenoxy side chain in Y187A resulted in a considerably larger 1260-fold decrease in k_{cat} and a 150-fold decrease in k_{cat}/K_m. The Y187F variant showed a 2-fold increase in both $^{D}k_{cat}$ and $^{D}k_{cat}/K_m$, suggesting that hydrogen atom abstraction is more rate-limiting in the variant. In contrast, the 3-fold decrease in $^{D}k_{cat}$ for the Y187A mutant compared to that of the wild-type enzyme suggests that a step in the mechanism other than hydrogen atom abstraction has now become rate-limiting.

Anaerobic Absorption Spectra of the Y187 Variants. Holo-OAM exhibits characteristic changes in its UV−visible spectrum upon substrate binding. Absorption decreases at 416 and 528 nm signify external aldimine formation and homolysis of the Co−C bond, respectively.[20] Notably, the cob(II)alamin species is not detected upon reaction of wild-type OAM with the physiological substrate because of the shortened lifetime of the ensuing radical intermediates. However, the binding of the inhibitor, 2,4-diaminobutyrate (DABA), to OAM results in the formation of a long-lived 2,4-diaminobutyryl-4-yl-PLP radical. External aldimine formation with 2,4-diaminobutyrate leads to the abstraction of hydrogen from its C4 atom by Ado$^{\bullet}$. The resulting lone electron on the C4 neighbors the imine linkage and is therefore readily delocalized through the conjugated π-system of the PLP pyridine ring. The formation of this overstabilized radical species leads to the accumulation of the cob(II)alamin species, which is denoted as a discrete absorbance peak at 470 nm.[20]

To examine the effects of the Y187 substitutions on substrate binding, Co−C bond homolysis, and cob(II)alamin buildup, anaerobic UV−visible binding spectra were obtained for each of the variants upon them being mixed with DL-2,4-diaminobutyrate and D-ornithine (Figure 3). The binding spectra obtained for the Y187F mutant were similar to those previously published for wild-type OAM.[20] Binding of both the substrate D-ornithine (Figure 3A) and DL-2,4-diaminobutyrate (Figure 3B) resulted in a decrease in absorbance at 416 nm, indicating transimination. Examination of the decrease in absorbance at 528 nm revealed that DL-2,4-diaminobutyrate induces a greater percentage of Y187F to undergo homolysis than does D-ornithine, consistent with the native enzyme.[20] In the cases of both DABA and D-ornithine, the degree of homolysis is reduced in Y187F compared to that in wild-type OAM. Figure 3B shows a small increase in absorbance at 470 nm indicating that the

dx.doi.org/10.1021/bi5006706 | *Biochemistry* 2014, 53, 5432−5443

persistent DABA−PLP radical still forms in Y187F and is coupled to the cob(II)alamin species.

The binding spectra of the Y187A mutant exhibited marked differences from those of both wild-type OAM and the Y187F mutant. While transimination is evident upon binding of DL-2,4-diaminobutyrate (Figure 3D) to Y187A, the small decrease in absorbance at 416 nm in Figure 3C indicates that transimination upon binding of D-ornithine is impaired in the Y187A mutant. Moreover, no cob(II)alamin species was detected upon mixing of Y187A with DABA, which could be attributed to the decreased stability of the PLP−DABA-derived radical species.

Aerobic Absorption Spectra of the Y187 Variants. Wild-type OAM shows aerobic inactivation rates of 0.4 and 1.6 min^{-1} (increase in absorbance at 358 nm) in the presence of D-ornithine and DL-2,4-diaminobutyrate, respectively.[21] The 4-fold difference in these rate constants is attributed to the inhibitor's ability to form an overstabilized organic radical that persists alongside the oxygen-sensitive cob(II)alamin species.[20,21] A rapid increase in absorbance at 358 nm, representing interception of the cob(II)alamin species by O_2 to form cob(III)alamin, was observed in the aerobic binding spectra of both Tyr187 mutants (Figure 4). In comparison to the wild-type rate, the rate of inactivation is decreased 4- and 7-fold in the Y187F mutant with DL-2,4-diaminobutyrate (0.38 min^{-1}) and D-ornithine (0.06 min^{-1}), respectively (Figure 5). In contrast, the Y187A mutant shows a higher O_2 inactivation rate with D-ornithine (0.19 min^{-1}), such that it approximates the rate of inactivation in the presence of DL-2,4-diaminobutyrate (0.21 min^{-1}). The increased rate of cob(III)alamin formation with the physiological substrate points to an increased sensitivity of the Y187A mutant to molecular oxygen.

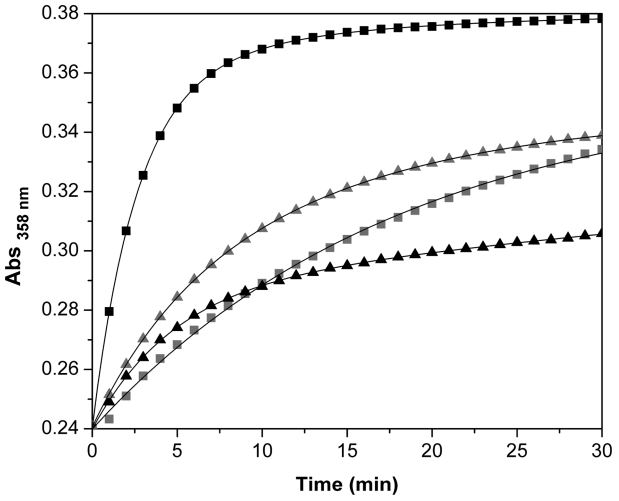

Figure 5. Rates of hydroxycobalamin formation in the Y187 variants. The rate of hydroxycobalamin formation was followed at 358 nm for Y187F (squares) and Y187A (triangles) upon reaction with DABA (black) and D-ornithine (gray). Data were fit to a double- or single-exponential equation to determine the observed rate constant for hydroxycobalamin formation. The Y187F mutant showed inactivation rates of 0.38 ± 0.01 and 0.06 ± 0.01 min^{-1} for DABA and D-ornithine, respectively. The Y187A mutant showed inactivation rates of 0.21 ± 0.01 and 0.19 ± 0.01 min^{-1} for DABA and D-ornithine, respectively.

Stopped-Flow Analysis of OAM and Y187 Variants. Pre-steady-state kinetic experiments with glutamate mutase and methylmalonyl-CoA mutase have shown that Co−C bond homolysis is coupled to hydrogen atom abstraction, such that reaction with their respective deuterium-labeled substrates causes a decrease in the observed rates of homolysis.[25,26] Reaction of holoOAM with D-2,4-diaminobutyrate-2,3,3,4,4-d_5 (360 ± 10 s^{-1}), however, yielded no discernible difference in the rate constant for Co−C bond homolysis from that observed upon reaction with protiated DL-2,4-diaminobutyrate (352 ± 7 s^{-1}) (Figure 6).

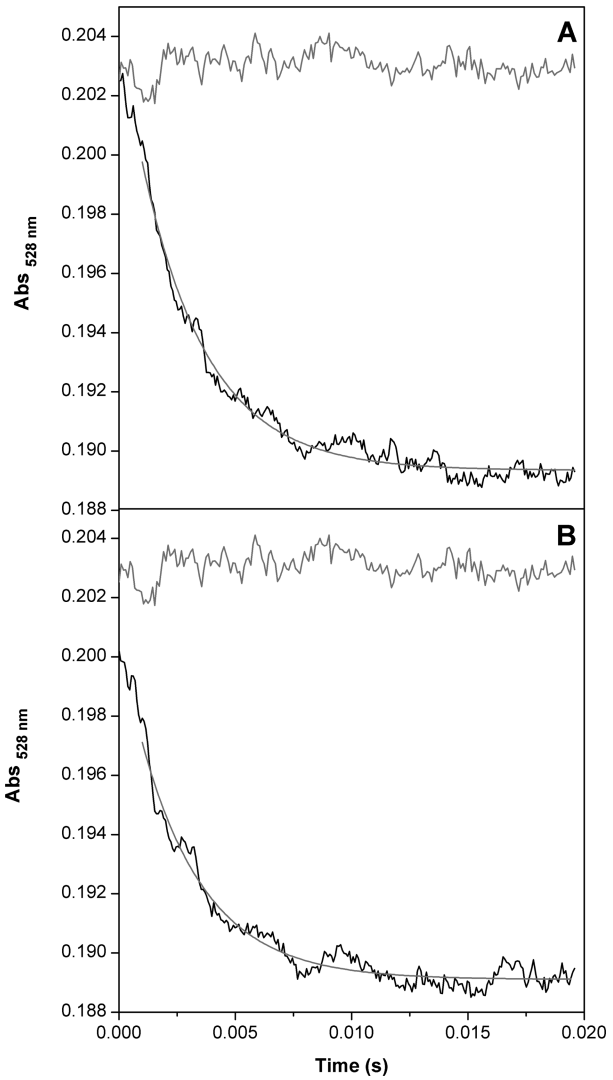

Figure 6. Stopped-flow absorbance changes following homolysis in wild-type OAM. Homolysis of the Co−C bond was monitored at 528 nm over 20 ms following rapid mixing of 50 μM holoOAM with 5 mM DL-2,4-diaminobutyric acid (A) and DL-2,4-diaminobutyric-2,3,3,4,4-d_5 acid (B) at 6.7 °C. In both cases, nine traces were averaged and fit to a single-exponential equation. The observed rate constant for homolysis in wild-type OAM was similar for DABA (352 ± 7 s^{-1}) and DABA-d_5 (360 ± 10 s^{-1}). Blank traces where holoOAM was rapidly mixed against buffer are shown in gray for reference.

Stopped-flow experiments were also performed with the Y187F and Y187A variants upon reaction with DL-2,4-diaminobutyrate to determine the effect of the mutations on the observed rate constants for Co−C bond homolysis and transimination. The rate constant for transimination was reduced 2- and 6-fold for Y187F (266 ± 4 s^{-1}) and Y187A (75 ± 1 s^{-1}), respectively (Figure 7), compared to that of the

dx.doi.org/10.1021/bi5006706 | Biochemistry 2014, 53, 5432−5443

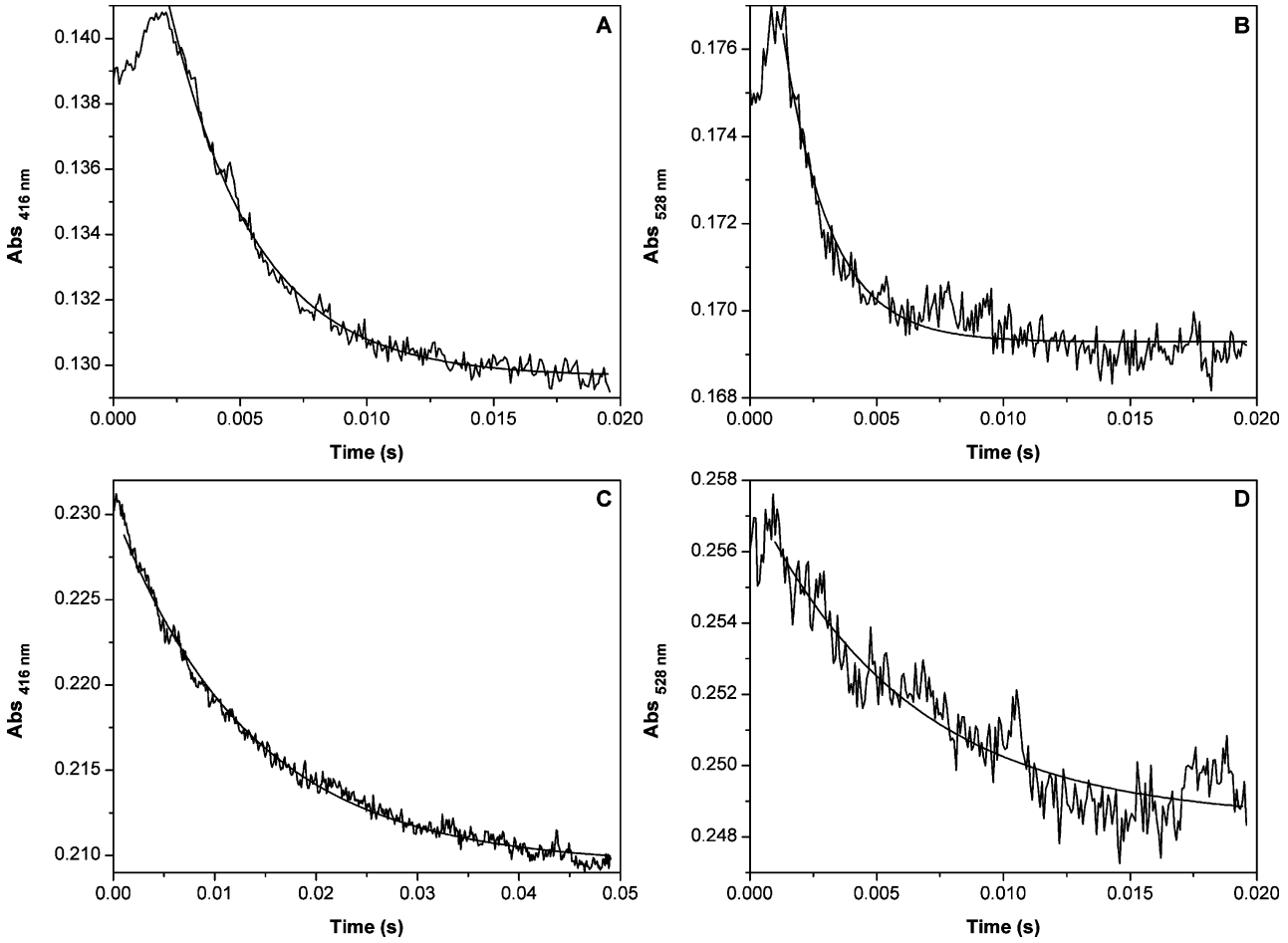

Figure 7. Stopped-flow absorbance changes following transimination and homolysis in the Y187 variants. Transimination and homolysis were monitored at 416 and 528 nm, respectively, following rapid mixing of 50 μM Y187F (A and B) and Y187A (C and D) with 5 mM DABA under anaerobic conditions at 25 °C. The rate constants for transimination were 266 ± 4 and 75 ± 1 s^{-1} for Y187F and Y187A, respectively. The rate constants for homolysis were 531 ± 19 and 165 ± 12 s^{-1} for Y187F and Y187A, respectively.

native enzyme.[20] The observed rate constant associated with the change in absorbance at 528 nm for the Y187F variant (531 ± 19 s^{-1}) was similar to that previously reported for wild-type OAM,[20] while that for Y187A was 3-fold slower (165 ± 12 s^{-1}). These results are consistent with the UV−visible spectral binding data (Figure 3), which showed smaller amplitude changes associated with external aldimine formation and Co−C bond homolysis for D-ornithine and DL-2,4-diaminobutyrate.

EPR Spectroscopy. An EPR signal is not observed upon reaction of native OAM with the natural substrate D-ornithine because of the shortened lifetime of the ensuing radical intermediates. However, the enzyme has previously been shown to exhibit an EPR signal with DL-2,4-diaminobutyrate because of the inhibitor's ability to form a persistent radical in the active site.[20] A simulation of the experimental EPR spectrum of wild-type OAM allowed the distance between the Co(II) center and the organic PLP radical to be estimated (Figure 8A). On the basis of the simulated value of *D*, the electron−electron dipole interaction, the distance between the two paramagnetic centers is approximately 7 Å. The shape of the EPR spectrum from the Y187F mutant is similar to that of the native enzyme with a major peak centered at $g\perp$ = 2.11 and well-resolved Co hyperfine splittings (Figure 8B). However, the 9-fold decrease in signal intensity indicates less radical formation, consistent with both the aerobic and anaerobic spectral studies for this OAM variant. No EPR signal was detected for the Y187A mutant upon reaction with DABA.

5,6-LAM Active Site Modeling. While crystal structures of OAM in both substrate-free and substrate-bound forms are available, only a resting-state crystal structure is available for 5,6-LAM.[10] To compare the substrate binding sites of OAM and 5,6-LAM, D-lysine and L-β-lysine were modeled into the 5,6-LAM active site using AutoDock. One hundred structures were generated for each simulation and clustered by conformational similarity (root-mean-square deviation within 2.0 Å). Structures were ranked in terms of energy from lowest to highest within each cluster. Each cluster was ranked on the basis of its lowest-energy structure (Figure S2 of the Supporting Informarion). For a structure to be considered a viable fit, the PLP portion of the ligand had to overlay with the original PLP cofactor in the substrate-free structure of 5,6-LAM.

The PLP−D-lysine simulation generated 31 distinct conformational clusters. The largest cluster consists of 20 structures and also contains the lowest-energy structure. Analysis of this lowest-energy structure reveals that the PLP portion of the ligand superimposes almost exactly with the original PLP cofactor, thereby retaining the numerous interactions between the enzyme and the phosphate group of PLP. The D-lysine portion of the ligand interacts primarily with two residues: Lys370 interacts with the α-carboxylate group,

dx.doi.org/10.1021/bi5006706 | *Biochemistry* 2014, 53, 5432−5443

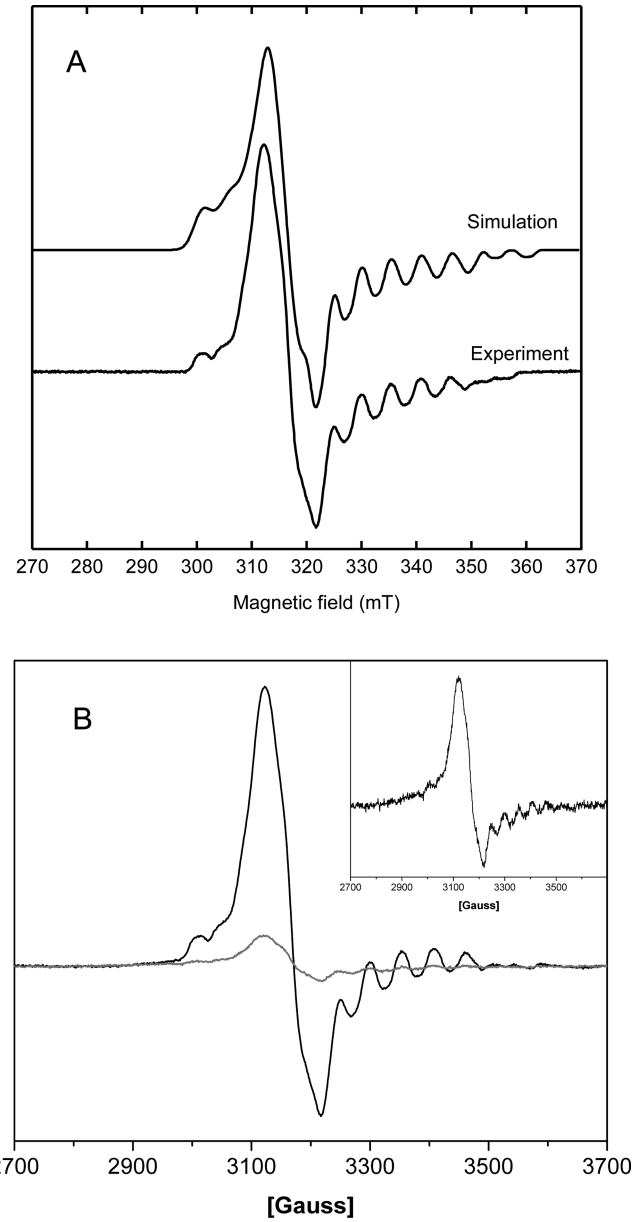

Figure 8. EPR spectra of holo-OAM and the Y187F mutant mixed with DL-2,4-diaminobutyric acid. (A) Experimental EPR spectrum and spectral simulation of wild-type OAM. Experimental parameters: frequency, 9.379 GHz; microwave power, 2 mW; time constant, 40.96 ms; modulation amplitude, 5 G; average of five scans of 120 s; temperature, 77 K. Simulation parameters: g(cobalamin) = [2.284, 2.233, 2.000], g(radical) = [2.001, 2.003, 2.001], J = −100 GHz, D = [−47.7, −146.7, 193.3] MHz, Euler angles D = [20, 5, −45]°, A(Co) = [0, 0.5, 12] mT, Euler angles of A(Co) = [−70, 25, 15]°, A(N) = [0, 0, 2] mT, Euler angles of A(N) = [0, 0, 0]°, line widths = [10, 10, 2] mT. (B) EPR spectrum of wild-type OAM (black), and on the same vertical scale the spectrum of Y187F (gray) showing decreased signal intensity. The shape of the Y187F spectrum (inset) is identical to that of wild-type OAM. Experimental parameters for the spectrum of Y187F were like those for wild-type OAM, except a frequency of 9.378 GHz.

while Asp298 interacts with the α-amino group (Figure 9A). Analogous interactions are observed in OAM. Arg297 in OAM replaces Lys370 of 5,6-LAM, while Glu81 replaces Asp298 (Figure 2). Similar results were obtained for the PLP−L-β-lysine simulation, which generated 25 distinct conformational clusters. The lowest-energy cluster contained 40 structures, including the lowest-energy structure. This lowest-energy structure retains all of the interactions observed with the PLP−D-lysine structure (Figure 9B).

DISCUSSION

Biochemical analyses of OAM and 5,6-LAM have revealed several mechanistic differences between these two homologues. First, 5,6-LAM is able to perform 1,2-shifts of three lysine isomers, whereas OAM is specific for D-ornithine. Second, recombinant 5,6-LAM undergoes rapid suicide inactivation involving direct transfer of an electron from cob(II)alamin to a substrate/product radical intermediate resulting in a buildup of cob(III)alamin and 5′-deoxyadenosine.[27] The spurious side reaction is insensitive to molecular oxygen and suggests that there are unique features of 5,6-LAM catalysis that compromise its ability to stabilize and control the trajectories of radical intermediates. Third, deuterium KIE and modeling studies suggest differences in substrate binding affinity for OAM and 5,6-LAM.

5,6-LAM elicits a high $^{D}k_{cat}$ value of 10.4 ± 0.3 and a $^{D}k_{cat}/K_m$ value of 8.3 ± 1.9, suggesting that hydrogen atom abstraction is the rate-limiting step of the mechanism.[28] In comparison, OAM presents an unusual case in which the value of $^{D}k_{cat}/K_m$ (2.5 ± 0.5) is smaller than the corresponding kinetic isotope effect on k_{cat} (7.6 ± 0.5). The magnitude of $^{D}k_{cat}$ suggests that hydrogen atom abstraction is at least partially rate-determining in the enzyme−substrate complex, while the difference in the values of $^{D}k_{cat}$ and $^{D}k_{cat}/K_m$ may be the result of a large forward commitment to catalysis in OAM. The value of k_{cat}/K_m includes all the rate constants of the mechanism from the binding of substrate up to and including the first irreversible step, which in the case of OAM is likely product release. k_{cat} on the other hand is independent of substrate binding and includes only those rate constants following formation of the enzyme−substrate complex. If an enzyme−substrate complex exhibits a stronger tendency to dissociate back into free enzyme and substrate rather than proceed forward through catalysis, then the values of $^{D}k_{cat}$ and $^{D}k_{cat}/K_m$ will be of a similar magnitude. However, if the rate of product formation is fast relative to the rate of dissociation of unreacted substrate from the enzyme, then the observed $^{D}k_{cat}/K_m$ value will be suppressed relative to $^{D}k_{cat}$.[29,30]

The suppression of the magnitude of the KIE on k_{cat}/K_m for OAM suggests that the substrate is "sticky" or has a relatively tight binding affinity for the active site. The crystal structure of OAM shows numerous noncovalent interactions with the substrate, including a bidentate ionic interaction between the α-carboxylate of D-ornithine and the guanidinium side chain of Arg297, a salt bridge between Glu81 and the α-amino group of the substrate, and a polar interaction between the imidazole side chain of His182 and the α-carboxylate of D-ornithine. Modeling of D-lysine and L-β-lysine into the active site of 5,6-LAM reveals fewer substrate−protein interactions. In 5,6-LAM, a single salt bridge to Lys370 replaces the Arg297 bidentate interaction with the α-carboxylate, the side chain of Asp298 replaces Glu81 in securing the α-amino group, and there is no corresponding residue for His182 in OAM. More noncovalent interactions between the protein and ornithinyl−PLP complex may result in a slower rate of release of substrate from the enzyme, thereby accounting for the suppressed KIE on $^{D}k_{cat}/K_m$. Fewer and weaker substrate interactions in 5,6-LAM likely increase the rate of substrate release relative to the rate of product formation (allowing for stronger expression of the KIE

dx.doi.org/10.1021/bi5006706 | Biochemistry 2014, 53, 5432−5443

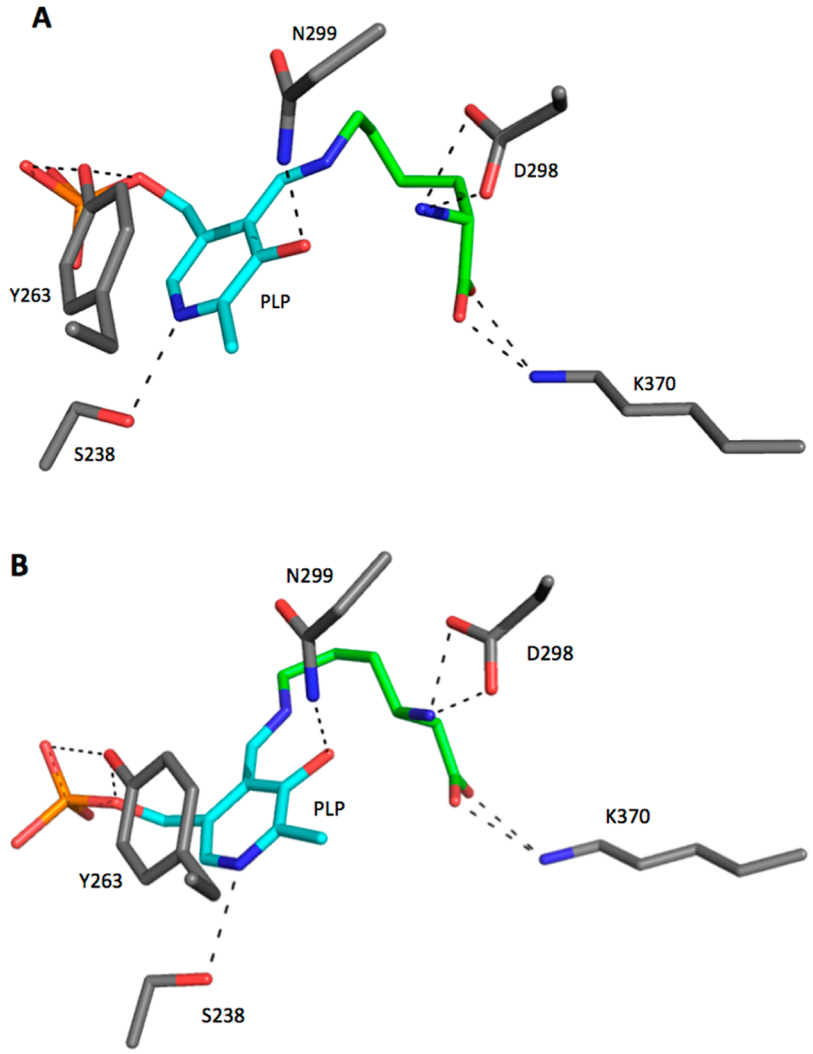

Figure 9. Model of the 5,6-LAM active site with bound substrate. 5,6-LAM with substrates D-lysine (A) and L-β-lysine (B) in the active site forming interactions with residues Lys370 and Asp298.

on $^{D}k_{cat}/K_m$) and could account for the enzyme's ability to accommodate different isomers of lysine into the active site.

KIE experiments with glutamate mutase and methylmalonyl-CoA mutase have shown that the rate constant for formation of cob(II)alamin is attenuated in the presence of deuterated substrate, indicating that Co−C bond homolysis is kinetically coupled to hydrogen atom abstraction.[25,26,31,32] While this is expected to be the case for class III aminomutases, our results revealed no decrease in the rate constant for homolysis upon reaction of OAM with deuterium-labeled DABA. At first glance, it would appear that homolysis is not in fact coupled to hydrogen atom abstraction in the aminomutases. However, given that homolysis is preceded by a transimination step, which exhibits a rate constant on the same order of magnitude, it is more likely that homolysis is kinetically "gated" by the formation of the external aldimine. Further evidence suggesting a gating mechanism is provided by stopped-flow experiments performed with the Y187F and Y187A mutants. Mutation of this residue to a Phe or Ala results in not only a decrease in the rate constant for transimination but also slower rates of Co−C bond homolysis even though the residue does not directly interact with the adenosylcobalamin cofactor. These data suggest that the decrease in absorbance observed at the adenosylcobalamin absorbance maximum (528 nm) reflects the rate of the preceding (and slower) transimination step, and that the rate constant for Co−C bond homolysis in native OAM is significantly faster than 500 s^{-1}.

We have also shown that Tyr187 is an important residue in OAM catalysis through its interaction with the PLP cofactor. In addition to the π-stacking interaction with the pyridine ring of PLP, Tyr187 also forms a hydrogen bond to the phosphate moiety of PLP via its hydroxyl group. Tyr263α makes identical contact with the PLP cofactor in the active site of 5,6-LAM. In 5,6-LAM, severing hydrogen bond contact with the phosphate group (enforced by a Y263F variant) obliterated catalytic activity.[19] In contrast, the corresponding mutation in OAM resulted in a 25-fold reduction in the rate of OAM turnover, while complete removal of the phenoxy side chain in Y187A reduced k_{cat} 1260-fold.

Pre-steady-state kinetic analysis revealed that mutation of Tyr187 leads to slight decreases in the rate constants for transimination, suggesting that the residue is involved in optimally positioning the PLP cofactor for external aldimine formation. UV−visible and EPR spectroscopy also reveal that the equilibrium between the intact AdoCbl cofactor and the organic radical and cob(II)alamin species is pushed toward the

dx.doi.org/10.1021/bi5006706 | *Biochemistry* 2014, 53, 5432−5443

reactants, indicating that Y187F and Y187A are less susceptible to Co−C bond homolysis. A high activation energy barrier for Co−C bond homolysis is also consistent with the elevated deuterium isotope effects on k_{cat} and k_{cat}/K_m observed for Y187F as it indicates that hydrogen atom abstraction is more, if not fully, rate-determining in the catalytic mechanism. The fact that $^{D}k_{cat}$ (16.7 ± 0.4) greatly exceeds the expected semiclassical limit of 7 indicates a dramatic increase in the probability of hydrogen tunneling in this OAM variant, and/or that the substitution unmasks the underlying contribution of tunneling to the observed KIE. A precedent for hydrogen tunneling in adenosylcobalamin-dependent enzymes has been set by temperature dependence studies of the kinetic isotope effects in both glutamate mutase[33] and methylmalonyl-CoA mutase.[34] In summary, the combined reductions in the rate constants for transimination, Co−C bond homolysis, and hydrogen atom transfer likely account for the pronounced decreases in the rates of catalytic turnover for the Tyr187 variants.

In 5,6-LAM, the Y263F mutation destabilizes the geometry of the active site, as the EPR spectrum shows a decoupling of the substrate-derived organic radical signal from that of the cob(II)alamin over an 8 min time frame.[19] The 5,6-LAM Y263F variant also appears to be more susceptible to O_2 inactivation. In contrast, the OAM Y187F variant is not more susceptible to O_2 inactivation (in fact, it is less so) and elicits an EPR spectrum that is identical in line shape to that of wild-type OAM. The intensity of the EPR signal is greatly reduced, but this is consistent with the UV−visible spectroscopic data that show a reduced level of cob(II)alamin formation. Thus, disruption of hydrogen bond contact with the PLP phosphate is less deleterious in OAM than in 5,6-LAM. While the Y187F mutation decreases the rate of transimination and radical initiation in OAM, it does not appear to distort the active site geometry, leading to a decoupling of the radical intermediates. This perhaps explains why the Y187F variant is not more susceptible to O_2 inactivation. In OAM, only once the tyrosine was replaced with a less conservative amino acid, alanine, did the enzyme become more susceptible to oxygen inactivation.

It is unclear why the mutation of the PLP-stacking tyrosine leads to differential effects on OAM and 5,6-LAM catalysis. A comparison of the EPR spectra of wild-type 5,6-LAM and OAM suggests that 5,6-LAM has a degree of active site flexibility that is increased compared to that of OAM. Reaction of 5,6-LAM with 4-thia-lysine results in the formation of an initial transient substrate radical species, which is located 7 Å from the cob(II)alamin center. Within 10 min, this transient radical tautomerizes into a more stable persistent radical, and in turn, the interradical distance increases to 10 Å.[35] In the case of OAM, the distance between the substrate-derived radical and the metal center is maintained at 7 Å. As such, the differential effects observed may be linked to active site architecture and the fact that OAM enlists more residues in securing the substrate within the active site. This extensive network of other noncovalent interactions may compensate for the effects of minor mutations, like Y187F. More tenuous substrate−protein interactions in 5,6-LAM likely support a broader substrate range, but they also offer a potential explanation for why this enzyme is more prone to suicide inactivation with the physiological substrate.

In summary, we have shown that the requirement of an additional cofactor to accomplish radical catalysis in the class III aminomutases results in kinetic gating of Co−C bond homolysis by the preceding transimination step of the mechanism. Through mutagenesis, we have also shown that the π-stacking interaction between Y187 and the pyridine ring not only optimally positions the PLP cofactor for formation of the external aldimine but also is essential for positioning the substrate relative to the adenosyl radical for effective hydrogen atom abstraction. Finally, we propose that weaker substrate binding interactions contribute to increased substrate promiscuity in 5,6-LAM, but at the cost of the enzyme being more prone to spurious radical side reactions. In comparison, a rigid active site in OAM leads to increased substrate specificity, as well as more controlled radical chemistry.

■ ASSOCIATED CONTENT

Supporting Information

Summary of steady-state kinetic parameters for wild-type OAM and the OAM variants upon reaction with deuterium-labeled substrate DL-ornithine-3,3,4,4,5,5-d_6 (Table S1), SDS−10% polyacrylamide gel showing purification of ornithine racemase (OR) from *C. difficile* by Ni-NTA affinity chromatography followed by Q-Sepharose anion exchange chromatography (Figure S1), and histograms of the 100 conformations generated in the D-lysine−PLP and L-β-lysine−PLP simulations conducted in AutoDock version 4.2.5.1 (Figure S2). This material is available free of charge via the Internet at http://pubs.acs.org.

■ AUTHOR INFORMATION

Corresponding Author

*Department of Chemistry, University of British Columbia Okanagan, 3333 University Way, Kelowna, BC V1V 1V7, Canada. E-mail: kirsten.wolthers@ubc.ca. Phone: (250) 807-8663. Fax: (250) 807-8009.

Funding

This work was supported by grants to C.J.W. and K.R.W. from the Natural Sciences and Engineering Research Council of Canada.

Notes

The authors declare no competing financial interest.

■ ACKNOWLEDGMENTS

We thank Dr. Paul S. Shipley, from the University of British Columbia Okanagan, for his assistance with NMR spectroscopy.

■ ABBREVIATIONS

AdoCbl, adenosylcobalamin; Ado$^{\bullet}$, 5′-deoxyadenosyl radical; AdoH, 5′-deoxyadenosine; OAM, ornithine 4,5-aminomutase; 5,6-LAM, lysine 5,6-aminomutase; PLP, pyridoxal 5′-phosphate; TIM, triosephosphate isomerase; DABA, DL-2,4-diaminobutyric acid; DABA-d_5, D-2,4-diaminobutyric-2,3,3,4,4-d_5 acid; DAP, 2,4-diaminopentanoic acid; DAPDH, 2,4-diaminopentanoic acid dehydrogenase; OR, ornithine racemase; NAD$^+$, β-nicotinamide adenine dinucleotide; EPPS, 4-(2-hydroxyethyl)piperazine-1-propanesulfonic acid; Tris, 2-amino-2-hydroxymethylpropane-1,3-diol.

■ REFERENCES

(1) Marsh, E. N., and Drennan, C. L. (2001) Adenosylcobalamin-dependent isomerases: New insights into structure and mechanism. *Curr. Opin. Chem. Biol.* 5, 499−505.

(2) Banerjee, R. (2003) Radical carbon skeleton rearrangements: Catalysis by coenzyme B12-dependent mutases. *Chem. Rev. 103*, 2083−2094.
(3) Fonknechten, N., Chaussonnerie, S., Tricot, S., Lajus, A., Andreesen, J. R., Perchat, N., Pelletier, E., Gouyvenoux, M., Barbe, V., Salanoubat, M., Le Paslier, D., Weissenbach, J., Cohen, G. N., and Kreimeyer, A. (2010) *Clostridium sticklandii*, a specialist in amino acid degradation: Revisiting its metabolism through its genome sequence. *BMC Genomics 11*, 555.
(4) Tsuda, Y., and Friedmann, H. C. (1970) Ornithine metabolism by *Clostridium sticklandii*. Oxidation of ornithine to 2-amino-4-ketopentanoic acid via 2,4-diaminopentanoic acid; participation of B12 coenzyme, pyridoxal phosphate, and pyridine nucleotide. *J. Biol. Chem. 245*, 5914−5926.
(5) Baker, J. J., Vanderdr, C., and Stadtman, T. C. (1973) Purification and Properties of β-Lysine Mutase, a Pyridoxal-Phosphate and B-12 Coenzyme Dependent Enzyme. *Biochemistry 12*, 1054−1063.
(6) Chang, C. H., and Frey, P. A. (2000) Cloning, sequencing, heterologous expression, purification, and characterization of adenosylcobalamin-dependent D-lysine 5,6-aminomutase from *Clostridium sticklandii*. *J. Biol. Chem. 275*, 106−114.
(7) Chen, H. P., Wu, S. H., Lin, Y. L., Chen, C. M., and Tsay, S. S. (2001) Cloning, sequencing, heterologous expression, purification, and characterization of adenosylcobalamin-dependent D-ornithine aminomutase from *Clostridium sticklandii*. *J. Biol. Chem. 276*, 44744−44750.
(8) Wolthers, K. R., Levy, C., Scrutton, N. S., and Leys, D. (2010) Large-scale domain dynamics and adenosylcobalamin reorientation orchestrate radical catalysis in ornithine 4,5-aminomutase. *J. Biol. Chem. 285*, 13942−13950.
(9) Dowling, D. P., Croft, A. K., and Drennan, C. L. (2012) Radical Use of Rossmann and TIM Barrel Architectures for Controlling Coenzyme B-12 Chemistry. *Annu. Rev. Biophys. 41*, 403−427.
(10) Berkovitch, F., Behshad, E., Tang, K. H., Enns, E. A., Frey, P. A., and Drennan, C. L. (2004) A locking mechanism preventing radical damage in the absence of substrate, as revealed by the X-ray structure of lysine 5,6-aminomutase. *Proc. Natl. Acad. Sci. U.S.A. 101*, 15870−15875.
(11) Ballinger, M. D., Frey, P. A., and Reed, G. H. (1992) Structure of a substrate radical intermediate in the reaction of lysine 2,3-aminomutase. *Biochemistry 31*, 10782−10789.
(12) Ballinger, M. D., Frey, P. A., Reed, G. H., and LoBrutto, R. (1995) Pulsed electron paramagnetic resonance studies of the lysine 2,3-aminomutase substrate radical: Evidence for participation of pyridoxal 5′-phosphate in a radical rearrangement. *Biochemistry 34*, 10086−10093.
(13) Wu, W., Lieder, K. W., Reed, G. H., and Frey, P. A. (1995) Observation of a second substrate radical intermediate in the reaction of lysine 2,3-aminomutase: A radical centered on the β-carbon of the alternative substrate, 4-thia-L-lysine. *Biochemistry 34*, 10532−10537.
(14) Miller, J., Bandarian, V., Reed, G. H., and Frey, P. A. (2001) Inhibition of lysine 2,3-aminomutase by the alternative substrate 4-thialysine and characterization of the 4-thialysyl radical intermediate. *Arch. Biochem. Biophys. 387*, 281−288.
(15) Mancia, F., Keep, N. H., Nakagawa, A., Leadlay, P. F., McSweeney, S., Rasmussen, B., Bosecke, P., Diat, O., and Evans, P. R. (1996) How coenzyme B12 radicals are generated: The crystal structure of methylmalonyl-coenzyme A mutase at 2 Å resolution. *Structure 4*, 339−350.
(16) Reitzer, R., Gruber, K., Jogl, G., Wagner, U. G., Bothe, H., Buckel, W., and Kratky, C. (1999) Glutamate mutase from *Clostridium cochlearium*: The structure of a coenzyme B12-dependent enzyme provides new mechanistic insights. *Structure 7*, 891−902.
(17) Makins, C., Pickering, A. V., Mariani, C., and Wolthers, K. R. (2013) Mutagenesis of a conserved glutamate reveals the contribution of electrostatic energy to adenosylcobalamin co-C bond homolysis in ornithine 4,5-aminomutase and methylmalonyl-CoA mutase. *Biochemistry 52*, 878−888.
(18) Wetmore, S. D., Smith, D. M., and Radom, L. (2001) Enzyme catalysis of 1,2-amino shifts: The cooperative action of B6, B12, and aminomutases. *J. Am. Chem. Soc. 123*, 8678−8689.
(19) Chen, Y. H., Maity, A. N., Pan, Y. C., Frey, P. A., and Ke, S. C. (2011) Radical Stabilization Is Crucial in the Mechanism of Action of Lysine 5,6-Aminomutase: Role of Tyrosine-263 α As Revealed by Electron Paramagnetic Resonance Spectroscopy. *J. Am. Chem. Soc. 133*, 17152−17155.
(20) Wolthers, K. R., Rigby, S. E., and Scrutton, N. S. (2008) Mechanism of radical-based catalysis in the reaction catalyzed by adenosylcobalamin-dependent ornithine 4,5-aminomutase. *J. Biol. Chem. 283*, 34615−34625.
(21) Makins, C., Miros, F. N., Scrutton, N. S., and Wolthers, K. R. (2011) Role of histidine 225 in adenosylcobalamin-dependent ornithine 4,5-aminomutase. *Bioorg. Chem. 40*, 39−47.
(22) Stoll, S., and Schweiger, A. (2006) EasySpin, a comprehensive software package for spectral simulation and analysis in EPR. *J. Magn. Reson. 178*, 42−55.
(23) Bothe, H., Darley, D. J., Albracht, S. P., Gerfen, G. J., Golding, B. T., and Buckel, W. (1998) Identification of the 4-glutamyl radical as an intermediate in the carbon skeleton rearrangement catalyzed by coenzyme B12-dependent glutamate mutase from *Clostridium cochlearium*. *Biochemistry 37*, 4105−4113.
(24) Fonknechten, N., Perret, A., Perchat, N., Tricot, S., Lechaplais, C., Vallenet, D., Vergne, C., Zaparucha, A., Le Paslier, D., Weissenbach, J., and Salanoubat, M. (2009) A Conserved Gene Cluster Rules Anaerobic Oxidative Degradation of L-Ornithine. *J. Bacteriol. 191*, 3162−3167.
(25) Padmakumar, R., Padmakumar, R., and Banerjee, R. (1997) Evidence that cobalt-carbon bond homolysis is coupled to hydrogen atom abstraction from substrate in methylmalonyl-CoA mutase. *Biochemistry 36*, 3713−3718.
(26) Marsh, E. N., and Ballou, D. P. (1998) Coupling of cobalt-carbon bond homolysis and hydrogen atom abstraction in adenosylcobalamin-dependent glutamate mutase. *Biochemistry 37*, 11864−11872.
(27) Tang, K. H., Chang, C. H., and Frey, P. A. (2001) Electron transfer in the substrate-dependent suicide inactivation of lysine 5,6-aminomutase. *Biochemistry 40*, 5190−5199.
(28) Tang, K. H., Casarez, A. D., Wu, W., and Frey, P. A. (2003) Kinetic and biochemical analysis of the mechanism of action of lysine 5,6-aminomutase. *Arch. Biochem. Biophys. 418*, 49−54.
(29) Northrop, D. B. (1975) Steady-State Analysis of Kinetic Isotope-Effects in Enzymic Reactions. *Biochemistry 14*, 2644−2651.
(30) Northrop, D. B. (1998) On the meaning of K-m and V/K in enzyme kinetics. *J. Chem. Educ. 75*, 1153−1157.
(31) Cheng, M. C., and Marsh, E. N. (2005) Isotope effects for deuterium transfer between substrate and coenzyme in adenosylcobalamin-dependent glutamate mutase. *Biochemistry 44*, 2686−2691.
(32) Yoon, M., Kalli, A., Lee, H. Y., Hakansson, K., and Marsh, E. N. (2007) Intrinsic deuterium kinetic isotope effects in glutamate mutase measured by an intramolecular competition experiment. *Angew. Chem. 46*, 8455−8459.
(33) Yoon, M., Song, H. T., Hakansson, K., and Marsh, E. N. G. (2010) Hydrogen Tunneling in Adenosylcobalamin-Dependent Glutamate Mutase: Evidence from Intrinsic Kinetic Isotope Effects Measured by Intramolecular Competition. *Biochemistry 49*, 3168−3173.
(34) Chowdhury, S., and Banerjee, R. (2000) Evidence for quantum mechanical tunneling in the coupled cobalt-carbon bond homolysis-substrate radical generation reaction catalyzed by methylmalonyl-CoA mutase. *J. Am. Chem. Soc. 122*, 5417−5418.
(35) Tang, K. H., Mansoorabadi, S. O., Reed, G. H., and Frey, P. A. (2009) Radical Triplets and Suicide Inhibition in Reactions of 4-Thia-D- and 4-Thia-L-lysine with Lysine 5,6-Aminomutase. *Biochemistry 48*, 8151−8160.